Commun. Theor. Phys. **73** (2021) 125501 (8pp) https://doi.org/10.1088/1572-9494/ac2f38

Ab initio calculation of the ground and first excited states of the lithium dimer

JianJun Qi[1], YuYao Bai[1], QianQian Guo[1], Yong-Chang Han[1,2] and Maksim B Shundalau[2,3]

[1] Department of Physics, Dalian University of Technology, Dalian 116024, China
[2] DUT-BSU Joint Institute, Dalian University of Technology, Dalian 116024, China
[3] Physics Department, Belarusian State University, Minsk, Belarus

E-mail: ychan@dlut.edu.cn

Received 29 August 2021, revised 12 October 2021
Accepted for publication 13 October 2021
Published 12 November 2021

Abstract

Based on a high level *ab initio* calculation which is carried out with the multireference configuration interaction method under the aug-cc-pVXZ (AVXZ) basis sets, X = T, Q, 5, the accurate potential energy curves (PECs) of the ground state $X^1\Sigma_g^+$ and the first excited state $A^1\Sigma_u^+$ of Li_2 are constructed. By fitting the *ab initio* potential energy points with the Murrell–Sorbie potential function, the analytic potential energy functions (APEFs) are obtained. The molecular bond length at the equilibrium (R_e), the potential well depth (D_e), and the spectroscopic constants (B_e, ω_e, α_e, and $\omega_e\chi_e$) for the $X^1\Sigma_g^+$ state and the $A^1\Sigma_u^+$ state are deduced from the APEFs. The vibrational energy levels of the two electronic states are obtained by solving the time-independent Schrödinger equation with the Fourier grid Hamiltonian method. All the spectroscopic constants and the vibrational levels agree well with the experimental results. The Franck–Condon factors (FCFs) corresponding to the transitions from the vibrational level ($v' = 0$) of the ground state to the vibrational levels ($v'' = 0$–74) of the first excited state have been calculated. The FCF for the vibronic transition of $A^1\Sigma_u^+(v'' = 0) \leftarrow X^1\Sigma_g^+(v' = 0)$ is the strongest. These PECs and corresponding spectroscopic constants provide reliable theoretical references to both the spectroscopic and the molecular dynamic studies of the Li_2 dimer.

Keywords: potential energy curve, spectroscopic constants, vibrational levels

(Some figures may appear in colour only in the online journal)

1. Introduction

Alkali metals are an important class of research prototypes in the fields of physics and chemistry [1–6]. The potential energy curves (PECs) play an important role in the calculation of molecular collision reactions, and hence, a large number of theoretical and experimental studies on the PECs of the alkali metal dimers have been performed [7, 8]. From the perspective of the electronic structure, the lithium dimer is the smallest homonuclear molecule in the alkali metal dimers. Therefore, much attention has been paid to the lithium dimer.

Many experimental studies on the electronic states and spectroscopic constants of Li_2 have been reported. Yiannopoulou studied the $2^3\Sigma_g^+$, $3^3\Sigma_g^+$, and $4^3\Sigma_g^+$ states of Li_2 using perturbation facilitated optical–optical double resonance (OODR) whose results of T_e and R_e were in very good agreement with the theoretical calculations [9]. Li *et al* observed the $3^3\Sigma_g^+$, $1^3\Delta_g$, and $2^3\Pi_g$ states of $^6Li^7Li$ by continuous wave perturbation facilitated OODR spectroscopy [10]. Other spectral techniques, for instance, all optical triple resonance (AOTR) etc, have also been applied to study Li_2 in experiment. Urbanski *et al* observed vibrational levels $v = 27$–62 and rotational levels ranging from $J = 0$ to 27 of the $A^1\Sigma_u^+$ state of Li_2 using AOTR [11].

The lithium dimer has also drawn enormous attention from theorists and a series of high level *ab initio* studies on Li_2 have been done in the past few decades. Halls *et al* used basis set of cc-pV5Z and the QCISD(T) method to calculate the lowest triplet excited state $a^3\Sigma_u^+$ [12]. Salihoglu *et al* employed two different quantum-mechanical models to obtain transition dipole moments for the $^7Li_2$ $A^1\Sigma_u^+ - X^1\Sigma_g^+$ system [13]. Musiał *et al* calculated selected spectroscopic

constants for 34 electronic states correlating to five lowest dissociation limits of Li_2 using FS-CCSD(2,0) method [14]. Chanana and Batra used symmetry adapted cluster configuration interaction theory and 6-311++G** basis set to calculate PECs and transition dipole moments of 22 states [15]. Lesiuk *et al* performed a composite method involving a six-electron coupled cluster and full configuration interaction theories combined with basis sets of Slater-type orbitals ranging in quality from double to sextuple zeta on the $A^1\Sigma_u^+$ state of Li_2 [16]. Fanthorpe *et al* reported level-resolved rate coefficients for collision-induced rotational energy transfer in the $^7Li_2$-Ne, with $^7Li_2$ in the high electronically excited $E^1\Sigma_g^+$ and $F^1\Sigma_g^+$ states [17].

There are also many studies about the ground state $X^1\Sigma_g^+$ of Li_2. Chanana *et al* calculated ground state properties of the Li_2 molecule in the presence of electric field using density functional theory [15]. Jasik and Sienkiewicz used the atomic effective core potential (ECP) with the self consistent field configuration interaction (SCF CI) method to calculate the $X^1\Sigma_g^+$ state [18]. The core electrons of Li atoms were represented by *l*-depended pseudopotential ECP2SD in their research, which did well for the excited states but was not good to describe the ground state. Nasiri and Zahedi calculated the PEC for the $X^1\Sigma_g^+$ of Li_2 by quantum Monte-Carlo method [19]. Most recently, Wang *et al* utilized the coupled cluster method including single and double substitutions and perturbative triples [CCSD(T)] with correlation consistent basis set to study the ground state of Li_2 [20]. In their calculations, the correlation effects of both the core and valance electrons were considered and their equilibrium bond length and potential well depth agreed well with experiment [21].

With the developments of the computational technology and the quantum chemistry methodology, it is possible for us to investigate the PECs of Li_2 with even more accurate theory and basis sets. Considering the limitation of single reference for CCSD(T), the multireference configuration interaction (MRCI) method is applied to the $X^1\Sigma_g^+$ and $A^1\Sigma_u^+$ states of Li_2 in this paper and all the six electrons will be considered in our method. Three different basis sets, aug-cc-pVXZ (AVXZ), X = T, Q, 5, are used for the *ab initio* calculations of single point energy, respectively. It is found that the results of AV5Z basis set are better than the others. The *ab initio* data points are fitted to the analytic Murrell–Sorbie potential function. Based on the fitted APEFs, the spectroscopic constants and vibrational energy levels of the two electronic states of the lithium dimer are obtained. The Franck–Condon factors (FCFs) for transitions between $v = 0$ of the $X^1\Sigma_g^+$ state and all the vibrational levels of the $A^1\Sigma_u^+$ state are also calculated. These two accurate PECs will provide a reliable reference for future experiments and theoretical calculations.

2. Computational details

2.1. Ab initio calculations

High level *ab initio* calculations are carried out by using the Molpro 2010 package [22]. We use the internally contracted MRCI method. Since the lithium dimer is a diatomic molecule with symmetry group $D_{\infty h}$ and there is only Abelian point group in the Molpro package, the largest subgroup D_{2h} of $D_{\infty h}$ is selected in our calculations. The D_{2h} point group includes $A_g/B_{3u}/B_{2u}/B_{1g}/B_{1u}/B_{2g}/B_{3g}/A_u$ irreducible representations. The augmented correlation consistent basis sets (aug-cc-pVXZ) (X = T, Q, 5) are employed to describe the lithium dimer. In the complete active space self-consistent field (CASSCF) calculations, ten molecular orbitals including three orbitals of A_g symmetry, one orbital of B_{3u} symmetry, one orbital of B_{2u} symmetry, three orbitals of B_{1u} symmetry, one orbital of B_{2g} symmetry, and one orbital of B_{3g} symmetry are chosen as the active space for the six electrons. Based on the CASSCF wave functions, we perform MRCI calculations at a series of given internuclear distances from 1.2 to 20 Å for the PECs of the $X^1\Sigma_g^+$ state and the $A^1\Sigma_u^+$ state of the lithium dimer with different basis sets.

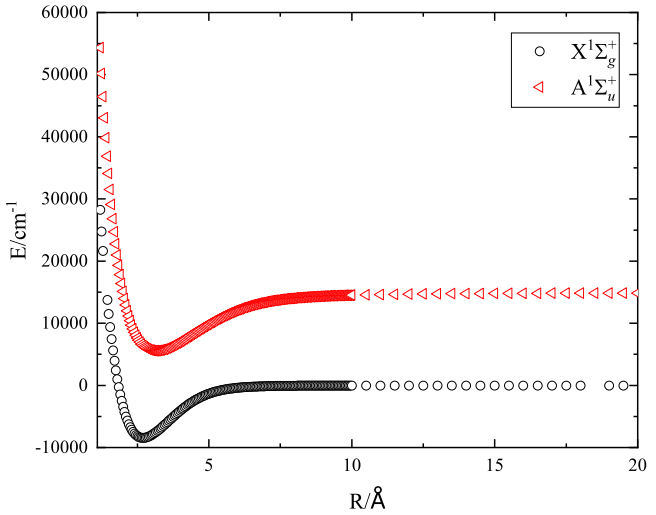

Figure 1. The *ab initio* energy points for the $X^1\Sigma_g^+$ and $A^1\Sigma_u^+$ states of the lithium dimer under the calculation of MRCI/AV5Z.

2.2. Potential energy functions

To construct an analytical potential energy function (APEF), many analytical function formulas have been proposed, such as Murrel–Sorbie (MS) [23], Tietz [24], and Wei [25] potential energy functions, etc. Among them, the MS potential energy function is widely and successfully applied in the construction of APEFs for many diatomic molecules [26–28]. The MS function can be described as [23]

$$V(\rho) = -D_e\left(1 + \sum_{i=1}^{n} a_i\rho^i\right)\exp(-a_1\rho), \tag{1}$$

where $\rho = R - R_e$, D_e is the potential well depth, R_e is the equilibrium bond length and R is the internuclear distance. The parameters D_e, R_e, and a_i can be determined by the nonlinear least square fitting method. In general, the accuracy of the MS function increases with the term number, n, and for light molecules, satisfactory results can usually be obtained when n is equal to 3 or 4 [26, 27]. However, because the values of the potential well depths of the $X^1\Sigma_g^+$ and $A^1\Sigma_u^+$ states of the lithium dimer are similar to some heavy diatomic

Table 1. The fitting parameters of the MS analytical potential energy functions for the $X^1\Sigma_g^+$ state based on MRCI/AVXZ (X = T, Q, 5) and the $A^1\Sigma_u^+$ state based on MRCI/AV5Z. The corresponding *ab initio* calculation values for R_e and D_e are listed in the parentheses.

Potential parameters	AVTZ $X^1\Sigma_g^+$	AVQZ $X^1\Sigma_g^+$	AV5Z $X^1\Sigma_g^+$	AV5Z $A^1\Sigma_u^+$
R_e/Å	2.6994 (2.6989)	2.6976 (2.6978)	2.6974 (2.6977)	3.1421 (3.1401)
D_e/cm^{-1}	8337.5346 (8338.6302)	8414.9678 (8416.1149)	8428.0893 (8429.2647)	9291.0809 (9290.2886)
$a1$/Å^{-1}	2.1776	2.1742	2.1729	1.5266
$a2$/Å^{-2}	1.6309	1.6239	1.6214	0.8087
$a3$/Å^{-3}	0.6373	0.6320	0.6305	0.2635
$a4$/Å^{-4}	0.1171	0.1149	0.1146	0.05164
$a5$/Å^{-5}	−0.027 57	−0.028 35	−0.028 30	0.009 509
$a6$/Å^{-6}	−0.014 67	−0.014 37	−0.014 34	0.000 7928
$a7$/Å^{-7}	0.002 564	0.002 635	0.002 566	−0.002 086
$a8$/Å^{-8}	0.001 453	0.001 395	0.001 388	0.000 1562
$a9$/Å^{-9}	0.000 1205	0.000 1292	0.000 1395	0.000 2391
a_{10}/Å^{-10}	−0.000 1254	−0.000 1253	−0.000 1269	−0.000 050 66
a_{11}/Å^{-11}	0.000 013 69	0.000 013 57	0.000 013 62	0.000 003 274
RMS/cm^{-1}	0.7672	0.8006	0.8166	2.7880

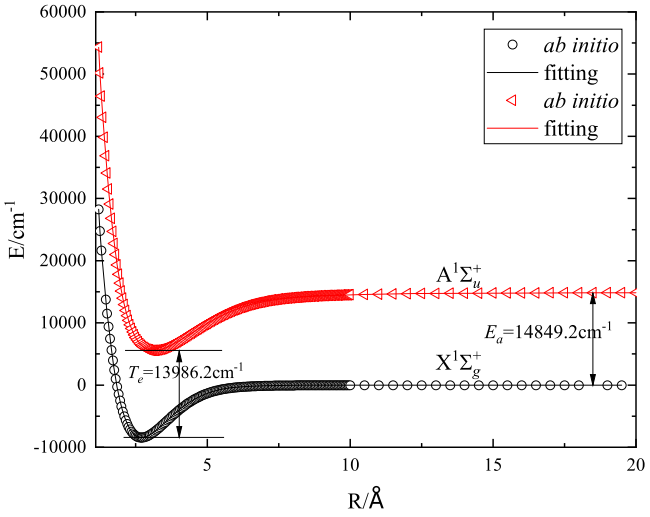

Figure 2. *Ab initio* points and fitting curves for the $X^1\Sigma_g^+$ and $A^1\Sigma_u^+$ states of Li_2 under MRCI/AV5Z; E_a is the atomic excitation energy and T_e is the adiabatic excitation energy.

molecules which have deep potential well [28, 29], we choose $n = 11$ to get satisfactory results after a series of attempts.

The spectroscopic constants could be obtained based on the MS function. The quadratic, cubic, and quartic force constants can be expressed as

$$f_2 = D_e(a_1^2 - 2a_2), \tag{2}$$

$$f_3 = 6D_e\left(a_1a_2 - a_3 - \frac{a_1^3}{3}\right), \tag{3}$$

$$f_4 = D_e(3a_1^4 - 12a_1^2a_2 + 24a_1a_3 - 24a_4), \tag{4}$$

and the spectroscopic constants are expressed as

$$B_e = \frac{h}{8\pi c\mu R_e^2}, \tag{5}$$

$$\omega_e = \sqrt{\frac{f_2}{4\pi^2\mu c^2}}, \tag{6}$$

$$\alpha_e = -\frac{6B_e^2}{\omega_e}\left(\frac{f_3R_e}{3f_2} + 1\right), \tag{7}$$

$$\omega_e\chi_e = \frac{B_e}{8}\left[\frac{-f_4R_e^2}{f_2} + 15\left(1 + \frac{\omega_e\alpha_e}{6B_e^2}\right)^2\right], \tag{8}$$

where μ is the reduced mass of Li_2, and c is the speed of light in vacuum. The spectroscopic parameters, B_e and α_e are the rotational constants at the equilibrium; ω_e and $\omega_e\chi_e$ are the harmonic vibrational frequency and the second term of vibrational constant, respectively.

3. Results and discussion

3.1. Analytical potential energy functions

For each basis sets (AVTZ, AVQZ, AV5Z), we calculate 194 and 198 energy points for the $X^1\Sigma_g^+$ and $A^1\Sigma_u^+$ states with R ranging from 1.2 to 20 Å, respectively. Generally, there are two approaches to increase the fitting accuracy. One is to optimize the distribution of the *ab initio* energy points by increasing the density of the energy points in the small R region where the interaction of the two atoms is strong. The other is to increase the fitting terms n of equation (1) to increase the accuracy with a high-order fitting function. Here, we adopt both approaches. The former is easy to achieve, and the latter is also computationally affordable for the diatomic molecular potential which only contains one dimension. To describe the important interaction region of the two atoms, we consider a dense grid for $R < 10$ Å with the grid gap of roughly 0.05 Å, while for the large internuclear distance of $R \geqslant 10$ Å, the sparse grid with the gap of roughly 0.5 Å is used. Taking the calculation of MRCI/AV5Z for example, the *ab initio* energy points for the two electronic states are presented in figure 1. The quantum chemical calculations for these energy points converge well, and the potential energy varies smoothly with the increase of R.

We obtain the APEFs of the ground and first excited states of Li_2 by fitting the *ab initio* energy points to equation (1) with

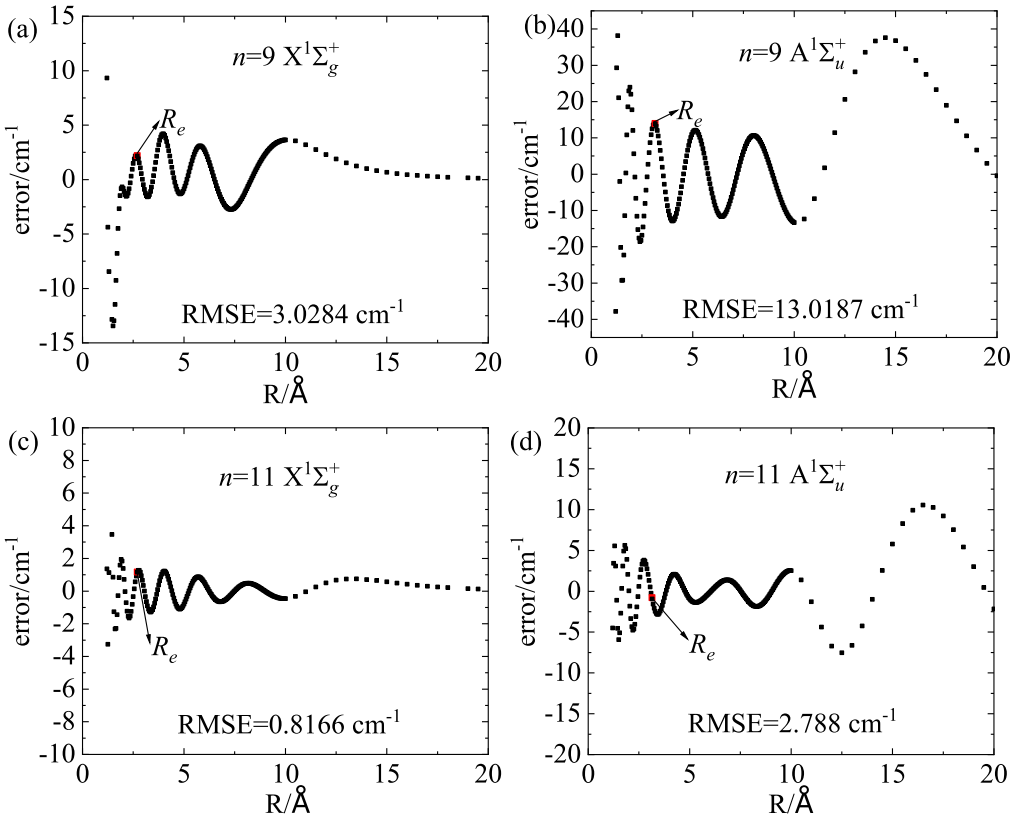

Figure 3. Fitting errors of the PECs for the ground state (a) and the first state (b) of Li_2 with $n = 9$; fitting errors of the PECs for the ground state (c) and the first state (d) of Li_2 with $n = 11$.

Table 2. Equilibrium bond lengths R_e (Å), potential well depth D_e (cm^{-1}) and spectroscopic constants (cm^{-1}) for the ground state $X^1\Sigma_g^+$ of Li_2.

Basis/References	R_e/Å	D_e/cm^{-1}	ω_e/cm^{-1}	B_e/cm^{-1}	$\omega_e\chi_e$/cm^{-1}	α_e/cm^{-1}
AV5Z	2.6974	8428.089	347.9251	0.661 04	2.4932	0.006 956
Exp. [21]	2.6734	8549.473	351.422 95	0.668 24	2.4417	—
Exp. [30]	2.673	8549.473	351.4	0.673	2.61	0.0068
Theory [18]	2.658	8613	352.41	—	—	—
Theory [34]	2.660	8510	353.0	—	—	—
Theory [35]	2.675	8466	351.01	—	—	—
Theory [19]	2.752	7856.64	352.50	0.675	2.70	—
Theory [14]	2.677	8466	351.0	—	—	—
Theory [38]	2.677	8065.541	351.9	0.671	2.56	0.0073
Theory [39]	2.7146	7307.38	327.50	0.668 24	2.651 47	0.006 50
Theory [33]	2.692	8297	347.1	—	3.6	—

Table 3. Equilibrium bond lengths R_e (Å), potential well depth D_e (cm^{-1}) and spectroscopic constants (cm^{-1}) for the state $A^1\Sigma_u^+$ of Li_2.

Basis/References	R_e/Å	D_e/cm^{-1}	ω_e/cm^{-1}	B_e/cm^{-1}	$\omega_e\chi_e$/cm^{-1}	α_e/cm^{-1}
AV5Z	3.142	9291.0809	253.704	0.487	1.511	0.005 02
Exp. [32]	3.108	9353.6079	255.47	0.498	1.581	0.005 48
Theory [36]	3.133	9366.5127	251.97	0.490	1.623	0.005 35
Theory [34]	3.094	9466	257.4	—	—	—
Theory [33]	3.13	9299	254	—	1.7	—
Theory [40]	3.072	9651.226	261.3	—	1.77	—
Theory [14]	3.112	9356	255	—	—	—
Theory [18]	3.092	9483	257.54	—	—	—

Table 4. The eigenenergies of vibrational levels for the ground state $X^1\Sigma_g^+$ of Li_2, relative to the bottom of the potential well (cm^{-1}).

Vibrational levels	$^7Li_2$	Exp. of $^7Li_2$ [21]	δ	$^6Li_2$	$^6Li^7Li$
0	173.945 07	175.032	0.62%	180.945 46	187.679 75
1	514.991 96	521.2611	1.20%	535.682 43	555.5745
2	851.009 63	862.2642	1.31%	884.9692	917.597 74
3	1181.955 78	1197.9974	1.34%	1228.757 25	1273.694 39
4	1507.7793	1528.4128	1.35%	1566.987 78	1623.797 43
5	1828.420 39	1853.4573	1.35%	1899.5918	1967.8281
6	2143.810 68	2173.0721	1.35%	2226.490 22	2305.695 88
7	2453.873 11	2487.1914	1.34%	2547.593 81	2637.298 48
8	2758.521 94	2795.7419	1.33%	2862.803 03	2962.521 61
9	3057.6625	3090.6412	1.07%	3172.007 88	3281.238 74
10	3351.191 03	3395.7978	1.31%	3475.087 47	3593.310 57
11	3638.994 29	3687.1094	1.30%	3771.909 67	3898.584 58
12	3920.949 17	3972.4624	1.30%	4062.330 54	4196.894 17
13	4196.922 17	4251.7309	1.29%	4346.193 57	4488.057 89
14	4466.768 81	4524.7756	1.28%	4623.328 95	4771.878 24
15	4730.3328	4791.4274	1.28%	4893.552 49	5048.140 41
16	4987.445 23	5051.5343	1.27%	5156.664 47	5316.610 74
17	5237.923 51	5304.9322	1.26%	5412.448 22	5577.034 79
18	5481.570 11	5551.3992	1.26%	5660.668 47	5829.135 24
19	5718.171 18	5790.7056	1.25%	5901.069 42	6072.609 25
20	5947.494 87	6022.6578	1.25%	6133.372 45	6307.1254
21	6169.289 37	6246.9482	1.24%	6357.2735	6532.320 18
22	6383.280 71	6463.314	1.24%	6572.439 91	6747.793 77
23	6589.170 09	6671.3979	1.23%	6778.506 85	6953.105 17
24	6786.6309	6870.8931	1.23%	6975.073 19	7147.766 69
25	6975.305 31	7061.4199	1.22%	7161.696 76	7331.237 74
26	7154.8003	7242.5556	1.21%	7337.889 15	7502.918 41
27	7324.6835	7413.8431	1.20%	7503.110 37	7662.143 36
28	7484.478 69	7574.8736	1.19%	7656.763 83	7808.178 19
29	7633.661 69	7724.9165	1.18%	7798.193 26	7940.221 94
30	7771.657 56	7863.7083	1.17%	7926.684 64	8057.423 82
31	7897.841 32	7990.4162	1.16%	8041.479	8158.929 24
32	8011.546 26	8104.473	1.15%	8141.807 58	8243.978 73
33	8112.0875	8205.2323	1.14%	8226.966 99	8312.078 42
34	8198.813 46	8292.0293	1.12%	8296.4519	8363.196
35	8271.200 14	8364.3066	1.11%	8350.124 34	8397.803 78
36	8328.9873	8421.6123	1.10%	8388.2943	8417.116 82
37	8372.291 21	8463.9648	1.08%	8411.709 99	8425.784 12
38	8401.576 36	—	—	8423.144 09	—
39	8418.019 85	—	—	8427.9374	—
40	8425.784 71	—	—	—	—

the fitting term number of $n = 11$. The fitting parameters for the PECs based on the *ab initio* energy points of AVTZ, AVQZ, and AV5Z are presented in table 1, respectively. R_e for the three sets of *ab initio* data are close to each other for the $X^1\Sigma_g^+$ state. However, D_e presents significant difference between the AVTZ and the AVQZ data ($\sim$80 cm^{-1}), while D_e for AVQZ and AV5Z are much closer ($\sim$14 cm^{-1}). Thus, out of the three bases, AV5Z is considered to be the most suitable for the lithium dimer. The corresponding fitting results for the $A^1\Sigma_u^+$ state with AV5Z basis set are listed in the last column of table 1. As shown in figure 2, the fitting curves for both the ground and excited states can well pass through all the *ab initio* energy points and the fitting curves are smooth with the variation of R. The adiabatic excitation energy (T_e) is 13 986.2 cm^{-1} which is close to the previous experimental report (14 068 cm^{-1}) [30]. The atomic excitation energy (E_a) is 14 849.2 cm^{-1} compared to the experiment (14 903 cm^{-1}) [31].

To further illustrate the validity of the MS fitting functions, we present the fitting error for each energy point in figure 3. Here, we compared two kinds of fittings: one is to set the term number n in the fitting function of equation (1) to be 9, and the other is to set $n = 11$. Obviously, with the increase of the term number, the fitting error decreases dramatically. The root means square (rms) errors can be calculated as $\mathrm{RMS} = \sqrt{\frac{1}{N}\sum_{i=1}^{N}(V_{\mathrm{APEF}} - V_{ab\ initio})^2}$, where N is the number of the data. As shown in figures 3(a) and (b), for $n = 9$, the rms = 3.0284 cm^{-1} for the $X^1\Sigma_g^+$ state is smaller than that (rms) for the $A^1\Sigma_u^+$ state. The distribution of the fitting error

Table 5. The eigenenergies of vibrational levels for the ground state $A^1\Sigma_u^+$ of Li_2, relative to the bottom of the potential well (cm^{-1}).

Vibrational levels	$^7Li_2$	Exp. of $^7Li_2$ [11]	δ	Vibrational levels	$^7Li_2$	Exp. of $^7Li_2$ [11]	δ
0	127.568 43	127.2989	0.21%	38	7428.303 59	7490.7088	0.83%
1	376.880 56	379.5847	0.72%	39	7552.610 13	7614.4744	0.81%
2	623.157 98	628.7628	0.90%	40	7672.434 98	7733.6054	0.79%
3	866.395 79	874.8276	0.97%	41	7787.653 52	7847.9802	0.77%
4	1106.592 87	1117.7878	1.01%	42	7898.142 05	7957.4828	0.75%
5	1343.751 17	1357.6575	1.03%	43	8003.781 36	8062.0058	0.72%
6	1577.875 08	1594.4510	1.05%	44	8104.461 43	8161.4558	0.70%
7	1808.9708	1828.1805	1.06%	45	8200.087 59	8255.7576	0.67%
8	2037.045 63	2058.8553	1.07%	46	8290.588 05	8344.8591	0.65%
9	2262.107 44	2286.4820	1.08%	47	8375.922 57	8428.7364	0.63%
10	2484.163 98	2511.0647	1.08%	48	8456.091 23	8507.398	0.60%
11	2703.222 39	2732.6056	1.09%	49	8531.141 77	8580.8882	0.58%
12	2919.288 62	2951.1052	1.09%	50	8601.173 15	8649.2902	0.56%
13	3132.366 96	3166.5620	1.09%	51	8666.3329	8712.7268	0.53%
14	3342.459 56	3378.9730	1.09%	52	8726.807 05	8771.36	0.51%
15	3549.566 06	3588.3326	1.09%	53	8782.803 46	8825.3883	0.48%
16	3753.683 18	3794.6329	1.09%	54	8834.532 03	8875.0421	0.46%
17	3954.804 38	3997.8627	1.09%	55	8882.186 98	8920.5765	0.43%
18	4152.919 62	4198.0072	1.09%	56	8925.936 07	8962.2626	0.41%
19	4348.015	4395.0479	1.08%	57	8965.920 77	9000.3768	0.38%
20	4540.0726	4588.9617	1.08%	58	9002.270 19	9035.1898	0.36%
21	4729.070 25	4779.7214	1.07%	59	9035.130 82	9066.9562	0.35%
22	4914.9813	4967.2950	1.06%	60	9064.709 43	9095.9063	0.34%
23	5097.774 47	5151.6462	1.06%	61	9091.312 89	9122.2439	0.34%
24	5277.413 68	5332.7340	1.05%	62	9115.350 98	9146.152	0.34%
25	5453.857 92	5510.5127	1.04%	63	9137.277 51	—	—
26	5627.061 02	5684.9326	1.03%	64	9157.499 54	—	—
27	5796.971 59	5855.9387	1.02%	65	9176.317 07	—	—
28	5963.532 81	6023.4718	1.01%	66	9193.9154	—	—
29	6126.6823	6187.4674	0.99%	67	9210.385 97	—	—
30	6286.352 01	6347.8558	0.98%	68	9225.749 96	—	—
31	6442.468	6504.5615	0.96%	69	9239.974 11	—	—
32	6594.950 43	6657.503	0.95%	70	9252.977 34	—	—
33	6743.713 35	6806.5922	0.93%	71	9264.627 73	—	—
34	6888.664 74	6951.7343	0.92%	72	9274.726 95	—	—
35	7029.706 44	7092.828	0.90%	73	9282.969 81	—	—
36	7166.734 29	7229.7651	0.88%	74	9288.831 93	—	—
37	7299.6384	7362.4316	0.86%	—	—	—	—

with the variation of R is also different between the two electronic states. The fitting error for the $X^1\Sigma_g^+$ state is large for the short R region ($R < 2$ Å) with the largest error of roughly 14 cm^{-1}, while the fitting for the $A^1\Sigma_u^+$ state presents large errors ($\sim$40 cm^{-1}) in both the short R region ($R < 2$ Å) and the asymptote region ($R > 10$ Å). This is because that the potential energy varies drastically in the short R region for both electronic states, and that potential energy of the $A^1\Sigma_u^+$ state presents a relatively long-range interaction to approaching the asymptote limit than the $X^1\Sigma_g^+$ state does. Nevertheless, the fitting error can be declined by increasing the fitting terms n. As shown in figures 3(c) and (d), for $n = 11$, the fitting errors for both states in all R region are appreciably smaller than those for $n = 9$. The fitting error for the $X^1\Sigma_g^+$ state for the short R region ($R < 2$ Å) has been decreased to within roughly 4 cm^{-1}. The fitting errors for the $A^1\Sigma_u^+$ state in the short R region ($R < 2$ Å) and the asymptote region ($R > 10$ Å) are now decreased to within 5 cm^{-1} and 10 cm^{-1}, respectively. These errors are actually considerable small compared to the deep well depths of the two states ($D_e = 8428\ cm^{-1}$ for $X^1\Sigma_g^+$ and $D_e = 9291\ cm^{-1}$ for $A^1\Sigma_u^+$). In addition, the fitting errors for the two states at the equilibrium R_e are both extremely small (1.176 cm^{-1} for $X^1\Sigma_g^+$ and 0.7788 cm^{-1} for $A^1\Sigma_u^+$). The rms errors for $n = 11$ and for different basis sets are also listed in table 1. The rms is 0.8166 cm^{-1} for the $X^1\Sigma_g^+$ state in our fitting to MRCI/AV5Z. Even for the $A^1\Sigma_u^+$ state, the rms is only 2.788 cm^{-1} which is much smaller than the permitted chemical accuracy (1.0 kcal mol^{-1} or 349.755 cm^{-1}) and proves the high quality of the fitting process. The small fitting error also indicates that the MS function is suitable for the description of the ground and first excited states of Li_2.

Hereinbefore, we demonstrate the fitting process and determine the APEFs with $n = 11$ based on the energy points calculated by MRCI/AV5Z. Now, we further compare the highly accurate fitting functions with previous reported

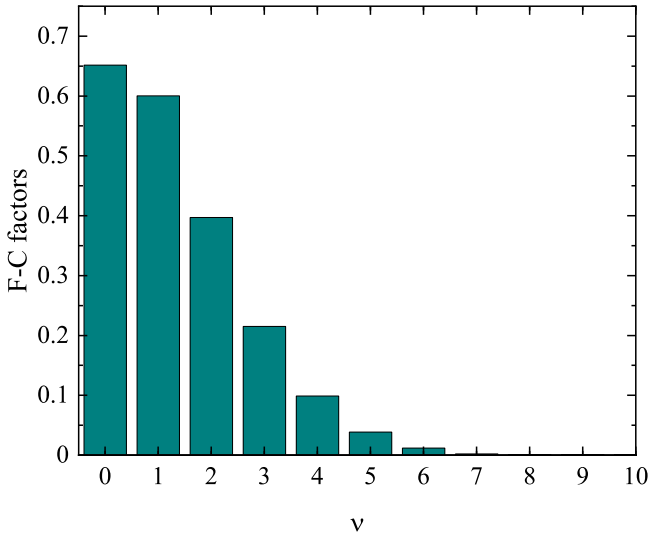

Figure 4. Franck–Condon factors for the transition from the $v' = 0$ of the $X^1\Sigma_g^+$ state to the $v'' = 0$–10 of the $A^1\Sigma_u^+$ state of $^7Li_2$.

spectroscopic constants in theory and experiment. The comparison for the $X^1\Sigma_g^+$ state is shown in table 2. Obviously, the values calculated from our APEFs, including the spectroscopic constants, equilibrium bond lengths R_e (Å), and potential well depth D_e (cm^{-1}) are all in good agreement with the experiments [21, 30], compared with previous theoretical reports [14, 18, 19, 33, 34, 38, 39]. The spectroscopic constants, equilibrium bond lengths R_e, and potential well depth D_e of the first excited state $A^1\Sigma_u^+$ are shown in table 3. It can be seen that the fitting APEFs for the excited state can also present accurate spectroscopic constants in good agreement with experimental and theoretical reports [14, 18, 32–34, 36, 40]. Thus, these APEFs based on MRCI/AV5Z for the ground and first excited states of the Li_2 dimer are reliable for future studies in spectroscopy and molecular dynamics.

3.2. Vibrational levels and FCF

Based on this newly constructed APEFs, we further calculated the vibrational energy levels by solving the following time-independent Schrödinger equation of nuclear motion using the Fourier grid Hamilton method [37].

$$\left[-\frac{\hbar^2}{2\mu}\frac{\mathrm{d}^2}{\mathrm{d}R^2} + \frac{j(j+1)\hbar^2}{2\mu R^2} + V^{(i)}(R)\right]\psi^{(i)}{}_{v,j}(R) = E^{(i)}{}_{v,j}\psi^{(i)}{}_{v,j}(R), \quad (9)$$

where μ is reduced mass, j is rotational quantum number, v is vibrational quantum number, and $V^{(i)}(R)$ is the APEF of the ith electronic state, $i = X^1\Sigma_g^+$ and $A^1\Sigma_u^+$.

Within the R range from 1.2 to 20 Å, we use 1024 grid points in the computation of the vibrational levels of the ground and first excited states of the lithium dimer. The density of the grid points has been checked to be converged by using even denser grids. The obtained vibrational levels (with $j = 0$) of the ground state of $^7Li_2$, $^6Li_2$, and $^6Li^7Li$ are listed in table 4, where δ is the relative difference between the present calculation and the previous experiment measurement [21]. The ground vibrational level of the $X^1\Sigma_g^+$ state is close to the experimental result with the rather small difference of 1 cm^{-1}. The relative difference δ for every vibrational level is less than 1.5%. In general, the APEF of the ground state of Li_2 from equation (1) is reliable. Due to the decrease of the reduced mass, the number of vibrational levels for $^6Li_2$ ($^6Li^7Li$) is smaller than that for $^7Li_2$, and for given vibrational level, the eigenenergy for the $^6Li_2$ ($^6Li^7Li$) dimer is higher than that for the $^7Li_2$ dimer.

The vibrational levels (with $j = 0$) of the first excited state $A^1\Sigma_u^+$ of Li_2 are listed in table 5. The differences between our calculations and the previous experimental reports for the vibrational levels of the $A^1\Sigma_u^+$ state are within 1.5%. Thus, the fitting APEFs for the two electronic states can also well describe the corresponding vibrational levels.

Based on the obtained vibrational level $v' = 0$ of the ground state and all the bound vibrational levels of the $A^1\Sigma_u^+$ state of

Table 6. Franck–Condon factors for the transition from the $v' = 0$ of the $X^1\Sigma_g^+$ state to the $v'' = 0$–74 of the $A^1\Sigma_u^+$ state of $^7Li_2$.

v''	F–C factors	v''	F–C factors
0	0.651 42	38	1.54E-10
1	0.600 29	39	7.65E-11
2	0.397 16	40	2.91E-11
3	0.214 89	41	2.24E-12
4	0.0988	42	1.16E-11
5	0.038 41	43	1.76E-11
6	0.0118	44	1.90E-11
7	0.002 01	45	1.81E-11
8	7.04E-04	46	1.61E-11
9	9.70E-04	47	1.38E-11
10	6.45E-04	48	1.15E-11
11	3.26E-04	49	9.41E-12
12	1.31E-04	50	7.63E-12
13	3.68E-05	51	6.15E-12
14	4.70E-07	52	4.94E-12
15	9.01E-06	53	3.97E-12
16	8.53E-06	54	3.18E-12
17	5.65E-06	55	2.56E-12
18	3.07E-06	56	2.06E-12
19	1.39E-06	57	1.66E-12
20	4.78E-07	58	1.34E-12
21	6.11E-08	59	1.09E-12
22	8.77E-08	60	8.90E-13
23	1.13E-07	61	7.30E-13
24	9.23E-08	62	6.10E-13
25	6.23E-08	63	5.10E-13
26	3.69E-08	64	4.30E-13
27	1.92E-08	65	3.70E-13
28	8.43E-09	66	3.10E-13
29	2.55E-09	67	2.70E-13
30	2.49E-10	68	2.30E-13
31	1.31E-09	69	1.90E-13
32	1.49E-09	70	1.60E-13
33	1.29E-09	71	1.40E-13
34	9.87E-10	72	1.10E-13
35	6.91E-10	73	9.00E-14
36	4.51E-10	74	6.00E-14
37	2.75E-10	—	—

Li_2, we calculate the corresponding FCFs, $\langle \Psi^X_{v'=0} | \Psi^A_{v''=0} \rangle$, which are illustrated in figure 4 and the specific values are listed in table 6. As seen in figure 4 and table 6, the maximum FCF corresponds to the overlap between $v' = 0$ and $v'' = 0$, and the value of FCF decreases dramatically with the increase of the vibrational quantum number v'' of the excited state. For v'' greater than 7, one cannot figure out its contribution from figure 4. It is because that the equilibriums for the PECs of the two electronic states are similar, roughly 2.7 and 3.1 Å and that the width and depth of the two potential wells are also comparable. Thus, the ground vibrational wavefunctions for two electronic states are similar in shape and position, which can present the largest FCF.

4. Conclusion

The PECs of the $X^1\Sigma_g^+$ and $A^1\Sigma_u^+$ states of Li_2 have been calculated by MRCI method based on different basis sets AVTZ, AVQZ, and AV5Z.

Based on the comparison among the three basis sets, we perform the nonlinear least square fitting to the MRCI/AV5Z energy points with MS potential energy function. The rms errors for the $X^1\Sigma_g^+$ and $A^1\Sigma_u^+$ states are 0.8166 cm^{-1} and 2.788 cm^{-1}, respectively. The equilibrium distance, potential well depth, spectroscopic constants, and vibrational energy levels described by the two APEFs are in good agreement with the experimental reports. The FCFs corresponding to the transitions from the vibrational level ($v' = 0$) of the ground state to the vibrational levels ($v'' = 0$–74) of the first excited state have been calculated, which indicates that the vibronic transition from $X^1\Sigma_g^+$ ($v' = 0$) to $A^1\Sigma_u^+(v'' = 0)$ is the strongest. These two accurate APEFs provide a theoretical basis for future studies in spectroscopy and molecular dynamics of the Li_2 dimer.

Acknowledgments

The project is supported by the National Key R&D Program of China No. 2018YFA0306503; the National Natural Science Foundation of China under Grant Nos. 21873016, 12174044; the International Cooperation Fund Project of DBJI No. ICR2105; the Fundamental Research Funds for the Central Universities (DUT21LK08).

ORCID iDs

Yong-Chang Han https://orcid.org/0000-0002-9800-9390

References

[1] Cui Y, Deng M, You L, Gao B and Tey M K 2018 *Phys. Rev.* A **98** 042708
[2] Bormotova E A, Kozlov S V, Pazyuk E A, Stolyarov A V, Skomorowski W, Majewska I and Moszynski R 2019 *Phys. Rev.* A **99** 012507
[3] Liu X-P, Yao X-C, Qi R, Wang X-Q, Wang Y-X, Chen Y-A and Pan J-W 2018 *Phys. Rev.* A **98** 022704
[4] Li J, Harter A K, Liu J, de Melo L, Joglekar Y N and Luo L 2019 *Nat. Commun.* **10** 855
[5] Ji Z H, Gong T, Zhao Y T, Li C L, Xiao L T and Jia S T 2020 *J. Quantum Spectrosc. Radiat. Transfer* **254** 107215
[6] Liu Y-X and Zhao B 2020 *Chin. Phys.* B **29** 023103
[7] Zhang L-L, Song Y-Z, Gao S-B, Xu J-H, Zhou Y and Meng Q-T 2016 *Can. J. Phys.* **94** 1259
[8] Arndt P T, Sovkov V B, Ma J, Pan X H, Beecher D S, Tsai J Y, Guan Y F, Lyyra A M and Ahmed E H 2019 *Phys. Rev.* A **99** 052511
[9] Yiannopoulou A, Urbanski K and Lyyra A M 1995 *J. Chem. Phys.* **102** 3024
[10] Li D, Xie F, Li L, Lazoudis A and Lyyra A M 2007 *J. Mol. Spectrosc.* **246** 180–6
[11] Urbanski K, Antonova S, Yiannopoulou A, Lyyra A M, Li L and Stwalley W C 1996 *J. Chem. Phys.* **104** 2813
[12] Halls M D, Schlegel H B, DeWitt M J and Drake G W F 2001 *Chem. Phys. Lett.* **339** 427–32
[13] Salihoglu O, Qi P, Ahmed E H, Kotochigova S, Magnier S and Lyyra A M 2008 *J. Chem. Phys.* **129** 174301
[14] Musiał M and Kucharski S A 2014 *J. Chem. Theory Comput.* **10** 1200–11
[15] Chanana G, Batra K and Prasad V 2019 *Comput. Theor. Chem.* **1169** 112620
[16] Lesiuk M, Musiał M and Moszynski R 2020 *Phys. Rev.* A **102** 062806
[17] Fanthorpe J, Gao Y X and Stewart B 2020 *J. Phys. Chem.* A **124** 7373–9
[18] Jasik P and Sienkiewicz J E 2006 *Chem. Phys.* **323** 563–73
[19] Nasiri S and Zahedi M 2015 *Chem. Phys. Lett.* **634** 101–7
[20] Wang Q-X, Wang Y-M, Ma R and Yan B 2019 *Acta Phys. Sin.* **68** 113102 (in Chinese)
[21] Barakat B, Bacis R, Carrot F, Churassy S, Crozet P, Martin F and Verges J 1986 *Chem. Phys.* **102** 215
[22] MOLPRO, version 2010.1, a package of *ab initio* programs, H-J Werner et al, see http://www.molpro.net/
[23] Murrel J N and Sorbie K S 1974 *J. Chem. Soc., Faraday Trans.* **2** 1552
[24] Tietz T 1963 *J. Chem. Phys.* **38** 3036
[25] Hua W 1990 *Phys. Rev.* A **42** 2524
[26] Ganguly G, Sen A, Mukherjee M and Paul A 2014 *Phys. Rev.* A **90** 012509
[27] Yang C-L, Zhu Z-H, Wang R and Liu X-Y 2001 *Theochem.—J. Mol. Struct.* **548** 47
[28] Gao F, Yang C-L, Wang J-H and Hu J-F 2009 *Theochem.—J. Mol. Struct.* **915** 193–7
[29] Zhang X-Y, Yang C-L, Gao F and Ren T-Q 2007 *Theochem.—J. Mol. Struct.* **816** 97–102
[30] Huber K P and Herzberg G 1979 *Molecular Spectra and Molecular Structure IV, Constants of Diatomic Molecules* (New York: Van Nostrand Reinhold) (https://doi.org/10.1007/978-1-4757-0961-2)
[31] Radziemski L J, Engleman R Jr and Brault J W 1995 *Phys. Rev.* A **52** 4462
[32] Kusch P and Hesse M M 1977 *J. Chem. Phys.* **67** 586
[33] Konowalow D D and Olson M L 1979 *J. Chem. Phys.* **71** 450
[34] Poteau R and Spiegelmann F 1995 *J. Mol. Spectrosc.* **171** 299–308
[35] Mink I S, Muller W and Meyer W 1985 *Chem. Phys.* **92** 263
[36] Shi D-H, Ma H, Sun J-F and Zhu Z-L 2007 *Commun. Theor. Phys.* **48** 1081–7
[37] Marston C C and Kurti G G B 1989 *J. Chem. Phys.* **91** 3571–6
[38] Jönsson B, Roos B O, Taylor P R and Siegbahn P E M 1981 *J. Chem. Phys.* **74** 4566
[39] Maniero A M and Acioli P H 2005 *Int. J. Quantum Chem.* **103** 711
[40] Konowalow D D and Fish J F 1984 *Chem. Phys.* **84** 463